Efficient Direct Measurement Mode Survey Test Procedure

Alvar M. Kabe*
The Aerospace Corporation, El Segundo, California

An efficient, direct measurement mode survey test procedure is presented. The procedure derives from the recognition that single-shaker frequency response functions of a linear, elastic structure can be scaled and summed to yield frequency response functions corresponding to multiple-shaker excitation. Thus, the operations to establish the multiple force levels needed to isolate modes for measurement can be performed numerically on a small laboratory computer/data acquisition system. In addition, this also introduces the possibility of numerically identifying mode parameters from single-shaker frequency response functions by using traditional sine-dwell testing techniques.

Nomenclature

b, c = modal contamination, Eq. (11) or (12)
$\{F\}$ = vector of elements F_ℓ or F_m
$[F]$ = matrix of elements $F_{\ell k}$
F_ℓ, F_m = excitation force amplitude at degrees-of-freedom ℓ or m
$f(t)$ = unit amplitude harmonic excitation force
$[I]$ = identity matrix
i = $\sqrt{-1}$
$[M]$ = mass matrix
$[\bar{M}]$ = unit normalized generalized mass matrix
Q_k = kth-mode modal force amplitude
$\{q(t)\}$ = vector of modal displacements
$\{\dot{q}(t)\}$ = vector of modal velocities
$\{\ddot{q}(t)\}$ = vector of modal accelerations
$\{x(t)\}$ = vector of physical displacements
$\ddot{x}_\ell(\omega)$ = acceleration frequency response of degree-of-freedom ℓ
α_{ef} = orthogonality between modes e and f
Ω' = real component of admittance, Eq. (6)
$i\Omega''$ = imaginary component of admittance, Eq. (7)
ω = frequency of excitation (rad/s)
ω_a, ω_b = half-power point frequencies (rad/s)
ω_n = natural frequency (rad/s)
$[\phi]$ = matrix of normal modes
$[\hat{\phi}]$ = shaker location mode shape estimates
$\phi_{\ell k}$ = kth-mode shape value at degree-of-freedom ℓ
$\{\phi^m\}_e$ = eth measured mode vector
$\{\phi\}_e$ = eth normal mode
ζ = critical damping ratio

Subscripts

e = mode number
f = mode number
i = iteration number
k = mode number
ℓ = physical coordinate number
m = counter for physical coordinates
r = number of physical coordinates
t = target mode, mode to be measured

Presented as Paper 87-0962 at the 28th AIAA/ASME/ASCE/AHS Structures, Structural Dynamics and Materials Conference, Monterey, CA, April 6-8, 1987; received May 26, 1987; revision received Nov. 30, 1987.

*Manager, Flight Loads Section, Structural Dynamics Department. Member AIAA.

Introduction

FORMULATION of accurate dynamic models of complex structures requires the experimental measurement of the structure's natural modes of vibration. A large number of test procedures and methodologies have been developed over the years to reduce the complexity and cost of establishing this data. These procedures can be categorized into those that measure the dynamic properties directly (e.g., Refs. 1-5) and those that identify the needed properties from frequency response functions or time domain free response data (e.g., Refs. 6-15). The decision as to which procedure to use is highly dependent on the test conditions and requirements.

The direct measurement procedures have several advantages. The principal advantage, however, is that the dynamic properties are measured directly. Thus, the disadvantage of interpreting numerical curve-fitting results, as required by the analytical mode identification procedures, is avoided. The principal disadvantage of the direct measurement procedures is that they are relatively time-consuming.

The most widely used direct measurement mode survey test procedure is the multishaker sine-dwell approach. The procedure consists of using one or more shakers to exert sinusoidally varying forces on the test article. The frequency of excitiation and the shaker force levels are adjusted to best isolate the target mode response from all other modes. Mode parameters are then established from direct measurement of the forced vibration.

Available sine-dwell test procedures that establish mode parameters by direct measurement require iterative adjustment of the shaker force levels and excitation frequency. The adjustment process is particularly time-consuming because shaker/structure interaction creates a need to adjust phase between the shaker force control signals to maintain colinear forces. This is further complicated when performing multishaker sine-sweeps since the phase between shaker forces will vary as a function of test article response. Frequency sweep results obtained without maintaining proper phasing of the forces are usually misleading and not indicative of the degree of mode isloation. An alternative is to perform a series of sine dwells and adjust the phase at each frequency. Obviously, this is time-consuming.

It is the purpose of this discussion to introduce a more efficient approach to multishaker sine-dwell mode survey testing. The procedure derives from the principle that the total response of a linear, elastic structure consists of the superposition of responses to the individual excitation sources. Assuming that linearity has been confirmed experimentally, frequency response functions obtained with single shakers can be

scaled and summed numerically to yield frequency response functions corresponding to multiple-shaker excitation. Thus, the adjustments to establish force levels needed to isolate each mode for measurement can be performed numerically. The final forces can then be applied to the structure and the entire mode vector measured.

This also introduces the possibility of identifying mode parameters from single-shaker frequency response functions using traditional multishaker sine-dwell testing techniques. To accomplish this, all that is required is that frequency response functions, corresponding to each excitation location, be measured for all accelerometer locations. Once the appropriate force levels for mode isolation have been established, all corresponding frequency response functions can be scaled and summed numerically. The mode parameters can then be obtained directly from the resulting multishaker equivalent frequency response functions.

Response to Harmonic Excitation

The behavior of a large class of linear, elastic structures subjected to multiple harmonic forces $\{F\}f(t)$ can be described in modal coordinates by the matrix differential equation of motion

$$[I]\{\ddot{q}(t)\} + [2\zeta\omega_n]\{\dot{q}(t)\} + [\omega_n^2]\{q(t)\} = [\phi]^T\{F\}f(t) \quad (1)$$

The coordinate transformation between physical coordinates $\{x(t)\}$ and modal coordinates $\{q(t)\}$ is

$$\{x(t)\} = [\phi]\{q(t)\} \quad (2)$$

and the matrix of mode shape vectors $[\phi]$ has been normalized with respect to the mass matrix such that

$$[\phi]^T[M][\phi] = [I] \quad (3)$$

Equation (1) consists of uncoupled second-order differential equations of the form

$$\ddot{q}_k(t) + 2\zeta_k\omega_{nk}\dot{q}_k(t) + \omega_{nk}^2 q_k(t) = \sum_{\ell=1}^{r} \phi_{\ell k}F_\ell f(t) \quad (4)$$

By solving Eq. (4) for each mode, the frequency response function for a typical physical coordinate can be obtained:

$$\ddot{x}_\ell(\omega)/f(\omega) = \sum_{k=1}^{r} \{\phi_{\ell k}(\Omega_k' + i\Omega_k'')Q_k\} \quad (5)$$

where

$$\Omega_k' = -\frac{\lambda_k^2[1-\lambda_k^2]}{[1-\lambda_k^2]^2 + [2\zeta_k\lambda_k]^2} \quad (6)$$

$$\Omega_k'' = \frac{2\zeta_k\lambda_k^3}{[1-\lambda_k^2]^2 + [2\zeta_k\lambda_k]^2} \quad (7)$$

$$Q_k = \sum_{\ell=1}^{r} \phi_{\ell k}F_\ell \quad (8)$$

$$\lambda_k = \omega/\omega_{nk} \quad (9)$$

In Eq. (5), the real part corresponds to the component of acceleration response that is colinear with the reference force time history, i.e., the coincident (Co) response. The imaginary part corresponds to the component of acceleration response that is 90 deg out of phase with the reference force time history, i.e., the quadrature (Qd) response. The term Q_k in Eq. (5) is the kth-mode modal force amplitude. The solution to Eq. (4) was obtained by establishing the particular solution corresponding to the modal force $Q_k e^{i\omega t}$. Equation (4), however, can also be solved by superposition of particular solutions corresponding to the individual terms that comprise $Q_k e^{i\omega t}$. Using this approach, the frequency response function for a typical physical coordinate is

$$\ddot{x}_\ell(\omega)/f(\omega) = \sum_{m=1}^{r} \{\sum_{k=1}^{r} \phi_{\ell k}(\Omega_k' + i\Omega_k'')\phi_{mk}F_m\} \quad (10)$$

Equations (5) and (10) yield equivalent frequency response functions. However, by using Eq. (10), the frequency response functions corresponding to each exciter are established individually. The superposition of these functions then yields the frequency response function corresponding to multiple-shaker excitation. The advantage of using Eq. (10) is that the response to a different set of force levels can be obtained by simply scaling the appropriate transfer functions and then summing them.

This suggests an efficient approach to multishaker sine-dwell mode surveying and introduces the possibility of using these techniques in a post-test mode identification procedure. Single-shaker excitation could be used to obtain frequency response functions for various locations of interest. The shaker can then be moved to another location (or another shaker can be used) and a new set of frequency response functions obtained. This can be repeated for several shaker locations. To obtain the frequency response functions corresponding to multiple-shaker excitation, all that is needed is that the appropriate functions be summed. Also, if different force levels are desired, the corresponding frequency response functions need only to be scaled before being added.

Isolation of Target Mode

Before introducing the mode identification procedure, a systematic approach to establishing the required force levels for mode isolation will be described. Practical aspects of mode-shape modal contamination, however, need to be addressed first.

Assume for the moment that the test article can be harmonically excited at all its degrees of freedom. Equation (5) indicates that the test article can be made to vibrate in a single normal mode by appropriately adjusting the shaker force levels F_ℓ such that the only nonzero modal force is that of the target mode. In practice, however, the number of degrees of freedom greatly exceeds the number of available shakers. Therefore, perfect isolation is not possible, and some degree of modal contamination will have to be accepted.

Modal contamination can be quantified by calculating the mass weighted orthogonality between measured mode vectors that have been normalized to unit modal mass. Let the "measured" mode vectors $\{\phi^m\}_e$ and $\{\phi^m\}_f$ consist of the quadrature components of total response and be defined as

$$\{\phi^m\}_e = \{\phi\}_e + b\{\phi\}_f \quad (11)$$

$$\{\phi^m\}_f = \{\phi\}_f + c\{\phi\}_e \quad (12)$$

The orthogonality α_{ef} between $\{\phi^m\}_e$ and $\{\phi^m\}_f$ is, therefore,

$$\alpha_{ef} = \{\phi^m\}_e^T[M]\{\phi^m\}_f / (\{\phi^m\}_e^T[M]\{\phi^m\}_e \{\phi^m\}_f^T[M]\{\phi^m\}_f)^{1/2} \quad (13)$$

$$= (b+c)/(1+c^2+b^2+b^2c^2)^{1/2} \quad (14)$$

$$\cong b+c \text{ for small } b \text{ and } c \quad (15)$$

It should be noted that contamination by additional modes would only introduce higher-order terms in Eq. (14). Thus, to a first approximation, Eq. (15) would still provide the mass weighted orthogonality between $\{\phi^m\}_e$ and $\{\phi^m\}_f$. This also

implies that valid orthogonality checks can only be obtained if all modes within the frequency range of interest are included in the check.

It is generally accepted in industry that mode shapes of acceptable quality have been measured if α_{ef} is less than 0.10. This requirement will be satisfied if

$$(\Omega_f''/\Omega_e'')(Q_f/Q_e) < b \tag{16}$$

$$(\Omega_e''/\Omega_f'')(Q_e/Q_f) < c \tag{17}$$

$$b + c < 0.10 \tag{18}$$

The preceding equations indicate that adequate mode isolation, from an off-resonance mode, will exist if the product of the quadrature admittance ratio and modal force ratio is less than b when $\{\phi^m\}_e$ is measured and less than c when $\{\phi^m\}_f$ is measured.

For lightly damped structures, the ratio (Ω_k''/Ω_t'') will decrease rapidly with increasing frequency separation between the two modes. Thus, careful attention to the applied forces, which determine the modal force ratio (Q_k/Q_t), is necessary only for modes close in frequency to the target mode. Since this is usually a small number, only a few shakers will be needed to satisfy the requirements of Eqs. (16), (17), and (18). Therefore, we shall proceed with the understanding that perfect isolation of a target mode is not necessary, and that adequate isolation can be achieved with a relatively small number of shakers.

In Ref. 4, Anderson formulated a systematic approach to isolate and measure modes using multishaker sine-dwell excitation. Anderson's procedure recognizes the natural selectivity of lightly damped structures to greatly decrease their quadrature response with increasing separation between the natural frequency and excitation frequency. Thus, as indicated by Eqs. (16) and (17), careful attention to the applied forces will generally be necessary only for modes in close frequency proximity to the target mode.

Data presented in Ref. 4 and practical test experience indicate that for lightly damped structures, generally only modes with frequencies within 10–15% of the target mode frequency need to be considered when measuring the target mode. To isolate the target mode response from these contaminating modes, Anderson proposed the selective orthogonal excitation (SOREX) test logic. The procedure consists of using successive estimates of mode-shape values to establish force vectors whose corresponding target-mode modal force is much larger than that of the modes close to it in frequency.

This is accomplished by establishing isolation groups of one or more target modes and all other modes within 10–15% in frequency. Shaker locations equal to the number of modes in the isolation group are then selected. Using single-shaker excitation, frequency response functions at the shaker locations are measured. From these transfer functions, estimates of shaker location mode-shape values are obtained. These approximate mode-shape amplitudes are then used to calculate the relative force levels to be applied with multiple shakers, i.e.,

$$[F]_{(i)} = ([\hat{\phi}]_{(i)}^T)^{-1} \tag{19}$$

The kth column of $[F]_{(i)}$ consists of the relative force levels to be applied by each shaker to improve the isolation of the kth mode. The subscript (i) designates the iteration number. The columns of $[\hat{\phi}]_{(i)}$ consist of the estimated mode shape values (quadrature components) for each shaker location. The kth column of $[\hat{\phi}]_{(i)}$ corresponds to the kth mode in the isolation group.

Each calculated force vector is then applied to the structure, the frequency of the excitation is adjusted to maximize quadrature response, and new mode-shape values at the shaker locations are measured. These values are then used in Eq. (19) to calculate a set of more refined forces. Typically, only one or two iterations are needed to obtain adequate isolation. Once this is achieved, the entire mode shape is measured.

Should an isolation group consist of more modes than there are available shakers, force patterns can still be obtained using a least-square error approximation:

$$[F]_{(i)} = ([\hat{\phi}]_{(i)}[\hat{\phi}]_{(i)}^T)^{-1}[\hat{\phi}]_{(i)} \tag{20}$$

The isolation of target modes will generally not be as complete, however, as when the number of shakers equals the number of modes in the isolation group. An example is presented in Ref. 4.

Mode Identification Procedure

A more efficient approach to multishaker sine-dwell testing than practiced heretofore will now be proposed. We will take the perspective that the procedure will be implemented on a small laboratory computer. It will be assumed that standard data acquisition and Fast Fourier Transform software are available as part of the total mode identification package to be described. Furthermore, we will assume that sufficient accelerometers have been deployed such that motions of all significant masses, and all resonant components, of all modes within the frequency range of interest, can be measured.

The first step is to acquire the needed frequency response functions. We begin by selecting a number of potential shaker locations. Then, using random or slow sinusoidal sweep excitation, we obtain frequency response functions associated with single-shaker forcing at each of these locations. It should be noted that it is also possible to obtain simultaneously several sets of frequency response functions, each associated with single-shaker excitation, by forcing the test article with multishaker uncorrelated random excitation (Refs. 16 and 17). If post-test mode identification is desired, frequency response functions for all accelerometers must be acquired. Otherwise, at this time, data is needed only for the potential multiple-shaker locations and any other coordinates whose response will aid in identifying all modes in the frequency range of interest.

These frequency response functions are then reviewed to determine preliminary natural frequencies. Mode isolation groups are established consisting of one or more target modes and any other modes sufficiently close in frequency to warrant inclusion in determining multiple excitation force levels. As discussed previously, all modes within 10–15% in frequency to the target modes should generally be included.

From the available shaker locations, those locations with strong resonances and phase reversals are selected for each isolation group. The number of shaker locations selected should equal the number of modes in the isolation group. Restricting our attention to one isolation group, we obtain for each mode in the group estimates of mode shape values at the selected shaker locations and form $[\hat{\phi}]_{(1)}$. Then, we use Eq. (19) to calculate the first iteration force levels, $[F]_{(1)}$. If fewer shaker locations than modes in an isolation group are available, Eq. (20) must be used.

The columns of $[F]_{(1)}$ are the force levels needed to better isolate each mode in the isolation group. Now, rather than applying these multiple-force levels to the test article and measuring new estimates of shaker location mode-shape values, we will take advantage of Eq. (10). For each mode in the isolation group, the following steps must be followed. First, we use the force levels from the appropriate column of $[F]_{(1)}$ to scale the corresponding transfer functions. Then, for each coordinate, we add these scaled frequency response functions.

For example, assume two shakers at locations ℓ and $\ell+1$ were selected, and the first iteration force levels, for the first

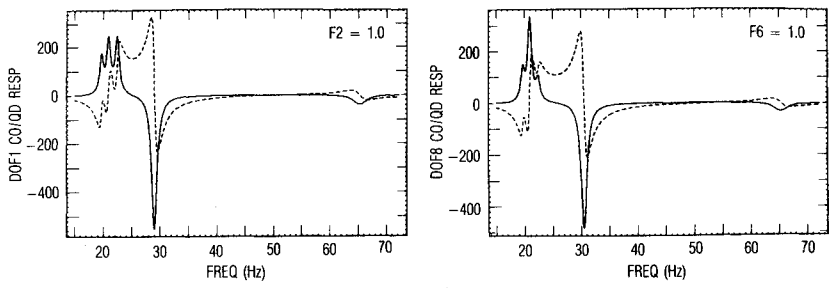

Fig. 1 Single-shaker excitation frequency response functions, coincident component ---, quadrature component —.

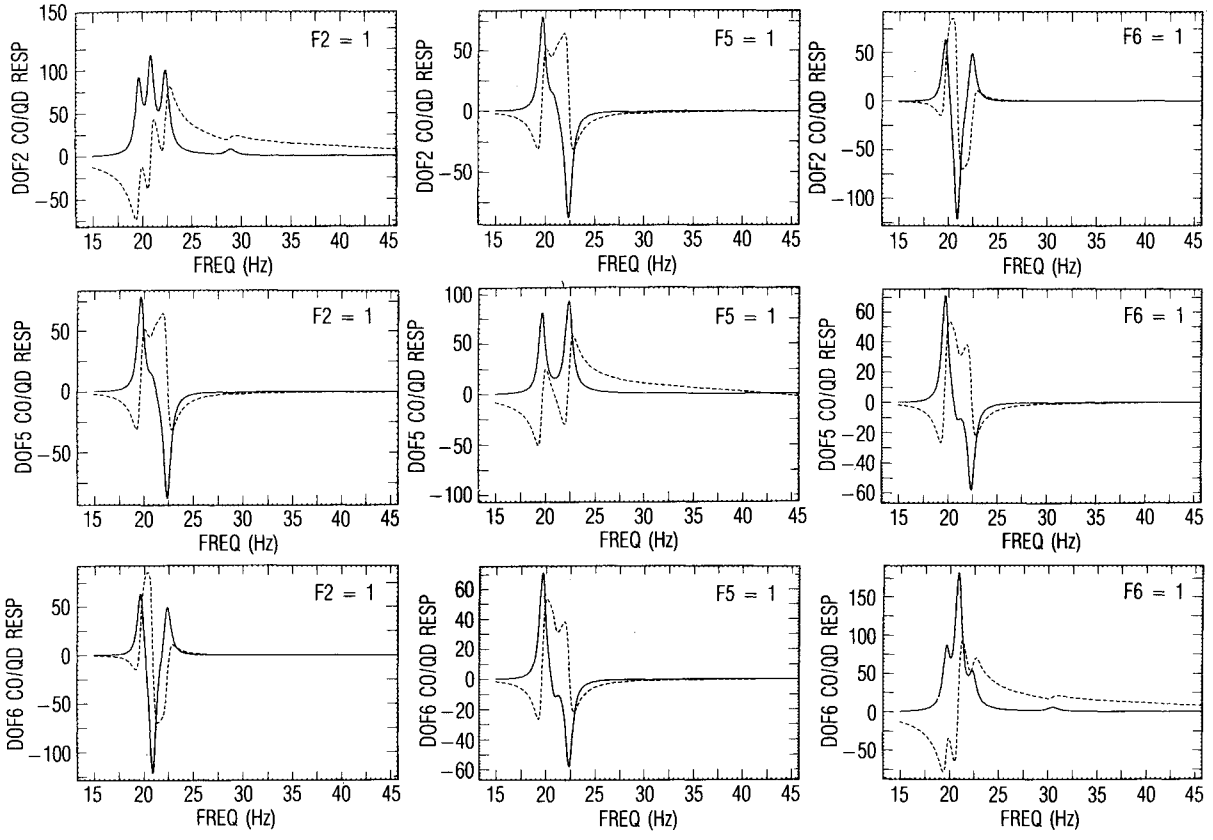

Fig. 2 Single-shaker coincident (---) and quadrature (—) frequency response functions for degrees of freedom 2, 5, and 6.

mode in the isolation group, are $F_{\ell,1}$ and $F_{\ell+1,1}$, respectively. Then, all frequency response functions corresponding to single-shaker excitation at location ℓ must be multiplied by $F_{\ell,1}$. Likewise, all frequency response functions associated with single-shaker excitation at location $\ell+1$ must be scaled by $F_{\ell+1,1}$. Finally, for each coordinate, the scaled frequency response functions are added. The resulting functions are equivalent to those that would be measured if the test article were excited simultaneously with $F_{\ell,1}$ and $F_{\ell+1,1}$.

These multishaker equivalent frequency response functions can then be reviewed to determine if adequate isolation has been achieved. If isolation is not adequate, better estimates of shaker location mode-shape values can be obtained from the new transfer functions. The given steps are repeated for each mode in the isolation group. This will yield new estimates for $[\hat{\phi}]_{(i)}$ and subsequently a new set of more refined forces, $[F]_{(i)}$.

Typically, only one or two iterations will be required to obtain the forces that will produce adequate isolation. The refined forces can then be applied to the structure, the frequency of excitation adjusted to maximize target mode quadrature response, and the entire mode vector measured. If frequency response functions were obtained for all accelerometer locations, the given scaling and summing operations could be performed for all coordinate locations. The mode shape is then obtained as the peak quadrature response, at ω_{nt}, from each transfer function. Thus, each mode shape can be isolated and recorded without collecting any additional data from the structure.

Table 1 Test article mass and upper triangular stiffness matrix elements

i,j	$k_{i,j}$	$M_{i,j}$	i,j	$k_{i,j}$	$M_{i,j}$
1,1	18	0.00055	5,5	6100	0.055
1,2	−18	— —	5,7	−200	— —
2,2	4118	0.055	6,6	4018	0.055
2,3	−4000	— —	6,7	−4000	— —
2,4	−100	— —	6,8	−18	— —
3,3	6100	0.055	7,7	6202	0.055
3,5	−100	— —	7,8	−2	— —
4,4	4100	0.055	8,8	20	0.00055
4,5	−4000	— —	— —	— —	— —

Damping should be obtained from the coincident response functions established in the final iteration using

$$\zeta_t = (\omega_a^2 - \omega_b^2)/4\omega_{nt}^2 \tag{21}$$

In this equation ζ_t is the critical damping ratio, ω_{nt} is the target mode natural frequency, and ω_a and ω_b ($\omega_a > \omega_b$) are the frequencies adjacent to ω_{nt} at which the coincident response peaks.

Numerical Simulation of a Test

To demonstrate the mode identification procedure, an analytical simulation of a test will be used. The "test article" mass and stiffness properties are presented in Table 1. The frequency response functions for single-shaker excitation were obtained using the closed-form complex solution to the equations of motion, Eq. (5). Critical damping ratios of 0.02 were assigned to each of the eight modes. Response values were calculated every 0.60 rad/s.

We begin the simulated test by exciting the structure with a single-shaker at coordinate X_2 and then at coordinate X_6. We process the response data at various coordinates into frequency response functions. Two of these transfer functions are presented in Fig 1. A review of this data indicates the presence of three modes in the 19–23 Hz range and two modes in the 28–32 Hz range. In this simulation we will restrict our attention to modes with frequencies below 50 Hz.

We will need two isolation groups. The first group will consist of the three modes in the 19–23 Hz range, and the second group will consist of the two modes in the 28–32 Hz range. Since the first group consists of three modes, three excitation locations must be selected. Data from two of these locations can then be used to isolate the two modes in the second group.

We select coordinates X_2, X_5, and X_6 for the multiple-excitation locations. We start by forcing the structure with a single shaker at coordinate X_2, and then process the response data at all eight coordinates into frequency response functions. The transfer functions for coordinates X_2, X_5, and X_6 are presented in column one of Fig. 2. We then excite the test article at coordinate X_5 and again establish frequency response functions for all eight coordinates. The functions for coordinates X_2, X_5, and X_6 are presented in the second column of Fig. 2. This is repeated a third time with excitation at coordinate X_6. The corresponding frequency response functions for coordinates X_2, X_5, and X_6 are presented in the third column of Fig. 2.

To establish the required multiple-shaker force levels, estimates of mode-shape values (quadrature components) at the shaker locations are needed. For the first isolation group, we will use the frequency response functions obtained with single-shaker excitation at coordinate X_6. The approximate mode-shape values are simply the peak quadrature response near the estimated natural frequency of each mode. If an obvious peak is not discernible, the value at the estimated frequency of the mode can be used.

The estimated shaker location mode-shape values are now used to form the truncated mode matrix $[\hat{\phi}]_1$. (The subscript denotes the iteration number.) For our three-mode isolation group, we obtain

$$[\hat{\phi}]_1 = \begin{bmatrix} 63.658 & -121.205 & 49.642 \\ 71.351 & -10.375 & 53.977 \\ 85.059 & 183.381 & 53.993 \end{bmatrix}$$

By substituting this matrix into Eq. (19), the multiple-excitation force levels $[F]_1$ needed to improve the isolation of each mode are obtained. The calculated force patterns, scaled to a maximum value of unity, are:

$$[F]_1 = \begin{bmatrix} 0.644 & -1.0 & 0.635 \\ 1.0 & -0.089 & -1.0 \\ 0.482 & 0.823 & 0.363 \end{bmatrix}$$

Next, we will establish the frequency response functions associated with the calculated multiple-shaker force levels. We begin with the force levels calculated for the first mode, i.e., the first column of $[F]_1$. First, we multiply the shaker location frequency response functions obtained with single-shaker excitation at coordinate X_2 (first column of Fig. 2) by $F_{2,1} = 0.644$ (the subscripts 2 and 1 denote the coordinate and mode number, respectively). Next, we multiply the functions obtained with single-shaker excitation at coordinate X_5 (second column of Fig. 2) and coordinate X_6 (third column of Fig. 2) by $F_{5,1} = 1.0$ and $F_{6,1} = 0.482$, respectively. Finally, for each coordinate (degree of freedom), the three scaled frequency response functions are summed. We repeat this procedure using the force levels calculated for the second mode and then the third mode.

The resulting frequency response functions for coordinate X_2 are presented in Fig. 3 (frequency response functions *b, c,* and *d*). These response functions are those that would be obtained if the multiple force levels in each of the three columns of $[F]_1$ were applied to the test article one set at a time. As can be ascertained from frequency response function *b*, isolation of the first mode relative to the other two modes has improved substantially. Likewise, response functions *c* and *d* indicate that the second and third modes are also much better isolated by the corresponding calculated force levels.

We can improve the mode isolation even further by calculating a new set of more refined force levels. First, we form a new truncated mode matrix,

$$[\hat{\phi}]_2 = \begin{bmatrix} 167.539 & -219.080 & 170.043 \\ 165.647 & -23.456 & -170.031 \\ 153.345 & 273.051 & 109.100 \end{bmatrix}$$

These refined shaker location mode-shape values were obtained from the multiple-excitation frequency response functions established with $[F]_1$. The shaker location mode shape values for the first mode were established from the frequency response functions obtained with the first coumn of $[F]_1$. The second and third mode values were obtained from the transfer functions corresponding to the second and third columns of $[F]_1$ respectively. By substituting the truncated mode matrix, $[\hat{\phi}]_{(2)}$ into Eq. (19), we obtain a refined set of force levels:

$$[F]_2 = \begin{bmatrix} 0.624 & -0.779 & 0.615 \\ 1.0 & -0.138 & 1.0 \\ 0.586 & 1.0 & 0.408 \end{bmatrix}$$

To obtain the frequency response functions associated with $[F]_2$, we repeat the scaling and summing operations as before. Note that these operations are to be performed on the original single-shaker data presented in Fig. 2. The resulting frequency response functions for coordinate X_2 are also presented in Fig. 3 and are labeled *e, f,* and *g*. A review of these three transfer functions indicates that the isolation of each target mode is adequate and that the entire mode vectors can now be established.

The determination of the force levels needed for mode isolation only involved the shaker location frequency response functions. Once the proper force levels are established, the frequency response functions associated with coordinates other than the shaker location coordinates can be scaled and summed as discussed. This operation only needs to be performed once, since the iterative part of the procedure

involves only the shaker location coordinates. The mode shapes can now be established by extracting from the multishaker equivalent frequency response functions the peak quadrature response at the natural frequency of the mode.

Having established the modes in the first isolation group, we can now proceed to the second group. There are two modes in this group; therefore, we will need two excitation locations. We select coordinates X_2 and X_6 since frequency response data already exists for these locations. From the transfer functions obtained with single-shaker excitation at coordinate X_2 (first column of Fig. 2), we obtain estimates of the mode shape values for the first of the two modes in the isolation group. For the second mode in the isolation group, we obtain estimates from the frequency response functions associated with single-shaker excitation at coordinate X_6 (third column of Fig. 2).

Next, we form for this isolation group the truncated mode matrix $[\hat{\phi}]_1$, i.e.,

$$[\hat{\phi}]_1 = \begin{bmatrix} 8.585 & 0.086 \\ 0.137 & 6.454 \end{bmatrix}$$

and use Eq. (19) to establish the required force levels $[F]_1$. These calculated forces, scaled to a maximum value of unity, are

$$[F]_1 = \begin{bmatrix} 1.0 & -0.016 \\ -0.013 & 1.0 \end{bmatrix}$$

The calculated force patterns, for all practical purposes, are equivalent to single-shaker excitation, and this is how in practice the modes should be excited. However, for the

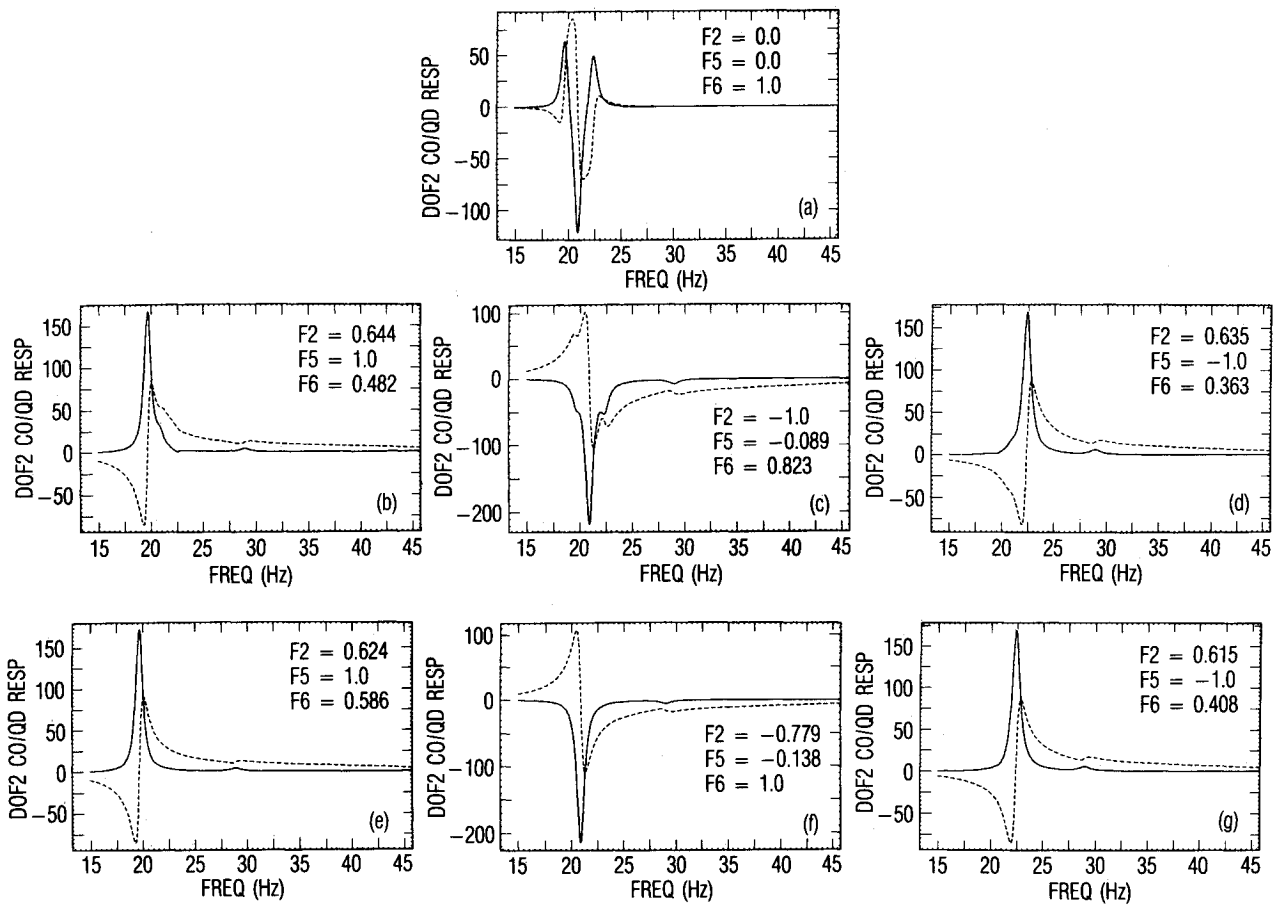

Fig. 3 Multiple-shaker equivalent coincident (---) and quadrature (−) frequency response functions for degree of freedom 2.

Table 2 Comparison of identified and exact mode shapes

	ϕ_1		ϕ_2		ϕ_3		ϕ_4		ϕ_5	
	Test	Exact	Test	Exact	Test	Exact	Test	Exact	Test	Exact
f_m	19.64	19.68	20.88	20.90	22.41	22.40	29.00	28.97	30.53	30.51
ζ	0.022	0.02	0.021	0.02	0.021	0.02	0.020	0.02	0.020	0.02
X_1	3.37	3.38	−4.29	−4.30	4.80	4.82	−41.73	−42.01	0.01	−0.03
X_2	1.80	1.80	−2.03	−2.03	1.90	1.90	0.65	0.53	0.005	0.004
X_3	1.40	1.40	−1.58	−1.58	1.48	1.48	0.58	0.50	0.004	0.003
X_4	2.25	2.25	−0.34	−0.34	−2.47	−2.47	−0.10	−0.07	−0.06	−0.05
X_5	1.79	1.79	−0.22	−0.22	−1.91	−1.91	−0.08	−0.05	−0.04	−0.02
X_6	1.68	1.67	2.64	2.64	1.23	1.23	0.01	0.01	0.56	0.46
X_7	1.32	1.32	2.00	2.00	0.89	0.89	0.004	0.003	0.49	0.42
X_8	2.83	2.83	4.89	4.89	2.63	2.63	0.09	0.06	−41.98	−42.18

Table 3 Summary of excitation forces and mode shape orthogonality

	Initial excitation					First iteration					Second iteration				
	ϕ_1	ϕ_2	ϕ_3	ϕ_4	ϕ_5	ϕ_1	ϕ_2	ϕ_3	ϕ_4	ϕ_5	ϕ_1	ϕ_2	ϕ_3	ϕ_4	ϕ_5
F_2	0.0	0.0	0.0	1.0	0.0	0.644	−1.0	0.635	1.0	−0.016	0.624	−0.779	0.615	1.0	−0.016
F_5	0.0	0.0	0.0	0.0	0.0	1.0	−0.089	−1.0	0.0	0.0	1.0	−0.138	−1.0	0.0	0.0
F_6	1.0	1.0	1.0	0.0	1.0	0.482	0.823	0.363	−0.013	1.0	0.586	1.0	0.408	−0.013	1.0
$[\bar{M}]$	1.00	0.21	0.07	0.01	0.01	1.00	−0.02	0.00	0.01	0.01	1.00	0.00	0.00	0.01	0.01
		1.00	0.21	−0.02	0.02		1.00	−0.01	−0.02	0.02		1.00	0.00	−0.02	0.02
			1.00	0.02	0.02			1.00	0.03	0.01			1.00	0.03	0.01
		SYM		1.00	0.03		SYM		1.00	0.00		SYM		1.00	0.00
					1.00					1.00					1.00

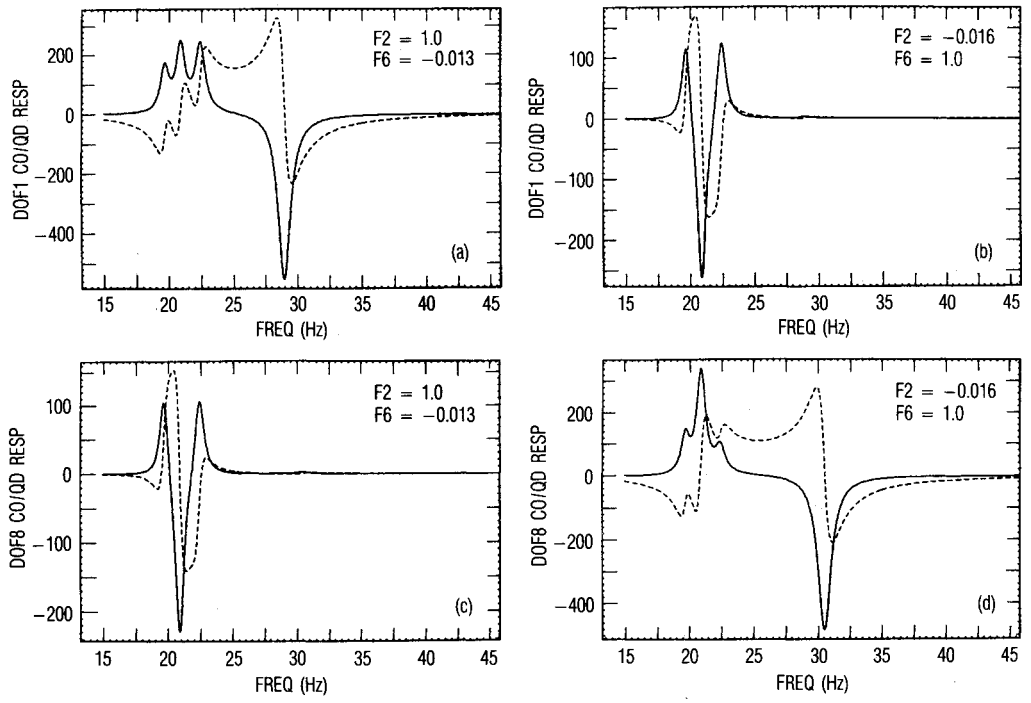

Fig. 4 Multiple-shaker equivalent coincident (---) and quadrature (−) frequency response functions for degrees of freedom 1 and 8.

purposes of this simulation we will repeat the frequency response function scaling and summing operations to establish the multishaker equivalent transfer functions. From these we can then extract the peak quadrature response values and establish the mode shapes.

The multishaker equivalent frequency response functions for coordinates X_1 and X_8 are presented in Fig. 4. Initially, it would appear that the three first modes of the system are contaminating the fourth and fifth modes. This is correct if one considers the coincident component of response as the measure of mode isolation. However, here we are only interested in the quadrature component when determining mode shapes and natural frequencies. Damping estimates only require, in addition to the natural frequency, the frequencies associated with the peaks of the coincident response. As can be observed in Figs. 4a and 4d, the frequencies at which these peaks occur are not affected significantly by contamination from the other modes.

The five identified mode shapes, natural frequencies, and damping values are compared to the true values in Table 2. As can be seen, close agreement exists between the identified values and the exact data. The mass weighted orthogonality of the five modes is presented in Table 3. The orthogonality of modes established with single-shaker excitation is presented in the column titled "Initial Excitation." The values in the column titled "First Iteration" correspond to modes established in the first iteration. The values in the last column correspond to the first three modes identified in the second iteration, whereas modes four and five are still the ones obtained in the first iteration. As this data indicates, the test success criterion of the mass weighted orthogonality between pairs of modes being less than 0.10 was satisfied after the first iteration.

Some Practical Considerations

A mode survey test is more difficult than the mathematical simulations would indicate. A primary concern in an actual test is the effect of the shakers on the dynamic properties of the test article. Lateral and rotational stiffnesses in the stingers should be minimized to the maximum extent possible. Furthermore, note that more consistent frequency response functions may result if the test article is forced with multishaker uncorrelated random excitation, since all the shakers will be attached to the structure at the same time.

Target mode isolation from modes not included in the isolation group is due primarily to frequency separation. Occasionally, however, the modal force of a mode not included in the isolation group is sufficiently large such that 10–15% frequency separation from the target mode is not sufficient. Although several corrective steps can be taken (see Ref. 5), the simplest is to include the contaminating mode in the isolation group, add another shaker location, and remeasure or reidentify the contaminated mode.

Numerical simulations are valuable research tools; however, the true test of a procedure occurs in the laboratory. In early 1985, the proposed procedure was used successfully

to improve the results of a multishaker sine-dwell test of a complex spacecraft structure. The procedure was used to remove two contaminating appendage modes from several measured primary structure modes. It is also encouraging that the results presented in Ref. 15 support the feasibility of combining scaled frequency response functions to improve mode isolation.

Summary

An efficient, direct measurement mode survey test procedure has been introduced. The procedure derives from the recognition that frequency response functions obtained with single shakers can be scaled and summed to yield frequency response functions corresponding to multiple-shaker excitation. Thus, the operations to establish force levels needed to isolate each mode for measurement can be performed numerically on a small laboratory computer/data acquisition system. The derived forces can then be applied to the structure and the entire mode vector measured. Thus, multiple-shaker excitation of the structure is not required until shaker locations and force levels have been established numerically.

The procedure introduced herein also can be used to numerically identify mode parameters from single shaker frequency response functions, with traditional multishaker sine-dwell testing techniques. All that is required is that frequency response functions, corresponding to each excitation location, be measured for all accelerometer locations. This quantity of data is already collected for many of the existing analytical mode identification procedures. Appropriate force levels can be established to isolate each mode, and all corresponding transfer functions then can be scaled and summed numerically. The mode parameters are established directly from the resulting multishaker equivalent frequency response functions. It should be noted, however, that this approach still needs to be tested with experimental data. In addition, as with any other mode survey test procedure, the test article should not be released until modes of acceptable quality have been established.

The numerical mode identification procedure presented herein has, in the opinion of the author, several advantages over other numerical curve fitting procedures. However, the principal advantage is that the dynamic properties are established directly from scaled, linear combinations of single-shaker frequency response functions. No analytical curve fitting is required. Thus, the disadvantage of interpreting numerical curve fitting results, as required by the existing post test mode identification procedures, is avoided. The proposed procedure will not yield computational modes since any mode to be identified has been selected by the engineer from a review of the raw frequency response function data.

References

[1]Lewis, R. C. and Wrisley, D. L., "A System for the Excitation of Pure Natural Modes of Complex Structures," *Journal of Aeronautical Sciences,* Vol. 17, Nov. 1950, pp. 705-722..

[2]Asher, G. W., "A Method of Normal Mode Excitation Utilizing Admittance Measurements," *IAS Proceedings of the National Specialists Meeting—Dynamics and Aeroelasticity,* Fort Worth, TX, Nov. 1958, pp. 69-76.

[3]Craig, R. R., Jr. and Su, Y. W. T., "On Multi-Shaker Resonance Testing," *AIAA Journal,* Vol. 12, 1974, pp. 924-931.

[4]Anderson, J. E., "Another Look at Sine-Dwell Mode Testing," *Journal of Guidance, Control, and Dynamics,* Vol. 5, July-Aug. 1982, pp. 358-365.

[5]Kabe, A. M., "Multi-Shaker Random Mode Testing," *Journal of Guidance, Control, and Dynamics,* Vol. 7, 1984, pp. 740-746.

[6]Kennedy, C. C. and Pancu, C. D. P., "Use of Vectors in Vibration Measurement and Analysis," *Journal of Aeronautical Sciences,* Vol. 14, Nov. 1947, pp. 603-625.

[7]Morosow, G. and Ayre, R. S., "Force Apportioning for Modal Vibration Testing Using Incomplete Excitation," *Shock and Vibration Bulletin,* Vol. 10, No. 48, Pt. 1, 1978, pp. 39-48.

[8]Stahle, C. V., Jr., "Phase Separation Technique for Ground Vibration Testing," *Aerospace Engineering,* July 1962, pp. 56-57, 91-96.

[9]Coppolino, R. N., "A Simultaneous Frequency Domain Technique for Estimation of Modal Parameters from Measured Data," Society of Automotive Engineers, Technical Paper Series 811046, Aerospace Congress and Exposition, Anaheim, CA Oct 5-8, 1981.

[10]Richardson, M. and Potter, R., "Identification of the Modal Parameters of an Elastic Structure from Measured Transfer Function Data," ISA ASI 74250, *20th International Instrumentation Symposium,* May 21-23, 1974, pp. 239-246.

[11]Richardson, M., "Modal Analysis Using Digital Test Systems," *Seminar on Understanding Digital Control and Analysis in Vibration Test System,* Part 2, Shock and Vibration Information Center, Naval Research Laboratory, Washington, D.C., May 1975, pp. 43-64.

[12]Vold, H., Kundrat, J., Rocklin, G. T., and Russell, R., "A Multi-Input Modal Estimation Algorithm for Mini-Computers," Society of Automotive Engineers, TP-820194, Feb. 1982.

[13]Ibrahim, S. R. and Mikulcik, E. C., "A Method for the Direct Identification of Vibration Parameters from the Free Response," *Shock and Vibration Bulletin,* Bulletin 47, Part 4, Sept. 1977, pp. 183-198.

[14]Juang, Jer-Nan and Pappa, R. S., "An Eigen System Realization Algorithm for Modal Parameter Identification and Model Reduction," *Journal of Guidance, Control, and Dynamics,* Vol. 8, Sept.-Oct. 1985, pp. 620-627.

[15]Brillart, R. and Hunt, D. L., "Computation of Total Response Mode Shapes Using Tuned Frequency Response Functions," *Proceedings of the Fourth International Modal Analysis Conference,* Union College, Schnectady, NY, 1986.

[16]Allemang, R. J., Rost, R. W., and Brown, D. L., "Dual Input Estimatio of Frequency Response Functions for Automotive Structure," Society of Automotive Engineers, TP-820193, Feb. 1982.

[17]Hunt, D. L. and Peterson, E. L., "Multishaker Broadband Excitation for Experimental Modal Analysis," Society of Automotive Engineers, Technical Paper Series 831435, Aerospace Congress and Exposition, Long Beach, CA, Oct. 3-6, 1983.